Rare Metal Materials and Engineering
Volume 53, Issue 10, October 2024
Available online at www.rmme.ac.cn

Science Press

Cite this article as: Deng Zhenzhen, Dai Zhengfei, Wu Weibo, et al. Corrosion Resistance of Titanium Bipolar Plate Enhanced by TiN Film[J]. Rare Metal Materials and Engineering, 2024, 53(10): 2755-2765. DOI: 10.12442/j.issn.1002-185X.20240194.

ARTICLE

Corrosion Resistance of Titanium Bipolar Plate Enhanced by TiN Film

Deng Zhenzhen[1], Dai Zhengfei[1], Wu Weibo[1], Lai Ruisi[1], Feng Qing[2], Jia Bo[2], Wang Chen[1], Lv Yuanjiang[1], Ma Fei[1]

[1] State Key Laboratory for Mechanical Behavior of Materials, Xi'an Jiaotong University, Xi'an 710049, China; [2] Xi'an Taijin Industrial Electrochemical Technology Co., Ltd., Xi'an 710021, China

Abstract: To improve the corrosion resistance of titanium (Ti) bipolar plate, titanium nitride (TiN) film was prepared on the surface of commercial TA1 pure titanium by magnetron reactive sputtering and pulse laser deposition (PLD) techniques, and the film prepared under different process parameters were evaluated. Results show that dense and complete TiN film can be obtained on TA1 surface under different preparation processes, and the corrosion current density of Ti substrate significantly increases. However, the composition of the film prepared by magnetron reactive sputtering is affected by the oxygen competition reaction, and its homogeneity is inferior to that of the film prepared by PLD. The comprehensive performance of the PLD-prepared film shows excellent characteristics in the terms of low corrosion current density (0.025 $\mu A \cdot cm^{-2}$), moderate corrosion overpotential (−0.106 V), and good hydrophobicity.

Key words: proton exchange membrane water electrolyzer; bipolar plate; process parameter; TiN film; corrosion resistance

Proton exchange membrane water electrolyzer (PEMWE) is a preferred high-quality equipment to produce hydrogen currently. It has the advantages of high current density, safe and reliable operation under high pressure environment, fast start-up speed, low operate temperature, and environmental friendliness[1]. The development of hydrogen energy is expected to solve two serious problems: global energy depletion and environmental pollution[2], which are beneficial to establish the low-carbon society[3–5]. Besides, hydrogen energy has broad application prospects in the fields of transportation, construction, energy storage, and industry. As the key component of PEMWE, bipolar plates serve multifaceted purposes, such as collecting current, separating oxidants, reducing agents, mechanical support, and uniform transportation of reaction media[6–7]. The bipolar plate accounts for about 70% of the overall PEMWE quality and 30% of the price of PEMWE equipment[8]. At present, there are many studies on the stainless steel bipolar plates[9–11] and light metal bipolar plates, such as titanium (Ti) [12–13], aluminum[14], and magnesium[15–16]. Among them, Ti has not only outstanding corrosion resistance but also lightweight characteristic, which can significantly improve the specific power of the stack. Therefore, Ti has good application prospects in PEMWE bipolar plates[17]. In the acidic environment of PEMWE, Ti induces the passivation effect. However, once Ti corrodes, it will release metal ions, which may poison the catalyst and proton exchange membrane[18], reducing the output power and operation life of PEMWE. Therefore, it is necessary to use conductive and corrosion-resistant materials to modify the surface of Ti-based bipolar plates[19–20]. Surface film is the most used modification method, and its preparation process generally involves chemical plating, electroplating, thermal spraying, physical vapor deposition, and chemical vapor deposition[21].

Currently, surface modification of Ti bipolar plates has become a research hotspot, and the films used for Ti plate modification mainly include metal-based and carbon-based films. Wang et al[22] used gilt Ti bipolar plates to effectively prevent and reduce the formation of oxide in membrane electrode components, which not only satisfied the corrosion resistance requirement, but also greatly reduced the interface

Received date: April 02, 2024
Foundation item: National Key Research and Development Program of China (2022YFB4002100)
Corresponding author: Ma Fei, Ph. D., Professor, State Key Laboratory for Mechanical Behavior of Materials, Xi'an Jiaotong University, Xi'an 710049, P. R. China, Tel: 0086-29-82668319, E-mail: mafei@mail.xjtu.edu.cn

contact resistance. However, the application of expensive platinum and gold cannot satisfy the commercial development. Shi et al[23] prepared a dense and undefective TiC-modified layer on the Ti plate surface by plasma surface modification technique. The corrosion current density of plate modified by TiC reduced by about an order of magnitude, compared with uncoated Ti plate, and the free corrosion potential significantly increased. Gao et al[24] prepared NbN coatings on Ti substrates by multi-arc ion plating technique and found that the corrosion current density was as low as 8.12 μA·cm^{-2}, and the maximum contact angle of the prepared coating could reach 100.0°. Compared with the unmodified Ti plate, the surface hydrophobicity of the modified Ti plate was significantly improved. However, these materials cannot be used for large-scale commercial application due to their inferior corrosion current density.

TiN, as a transition metal nitride, is a type of material with excellent properties and wide applications. Due to its high conductivity, excellent stability, good compatibility with Ti, and low cost, TiN is one of the commonly used coating materials for the modification of Ti bipolar plates of PEMWE[25]. However, the specific process and processing parameters are still obscure.

Therefore, in this research, magnetron reactive sputtering and pulse laser deposition methods were used to prepare TiN film on Ti substrate for surface modification, and the influence of process parameters on the corrosion resistance of TiN film was investigated. The differences in corrosion resistance of TiN film prepared under different process conditions were analyzed, providing experiment reference for surface modification of Ti bipolar plates of PEMWE and laying the preparation foundation for the bipolar plates with low-cost, high corrosion resistance, and long service life.

1 Experiment

In this research, commercial Ti plate TA1 (Ti substrate) with thickness of 1 mm was used as the experiment material. The element composition and content are shown in Table 1. All samples were ground by SiC sandpapers of 240#, 600#, 1000#, 2000#, and 3000#, and then polished to mirror-like state by diamond polishing paste with particle size of 0.5 μm. Then, the polished samples were ultrasonically cleaned with acetone, alcohol, and deionized water for 15 min, separately. Finally, all samples were dried in the air.

The film was prepared by magnetron reactive sputtering through the JGP450 high vacuum magnetron sputtering thin film deposition system. The sputtering schematic diagram is shown in Fig. 1a. The cathode used 99.9% Ti. When the vacuum degree of the chamber reached 5×10^{-4} Pa, the deposition process was initiated. The high purity Ar was introduced into the chamber at 20 mL/min throughout the entire process, and the parameters, such as N_2 flow rate, substrate temperature, sputtering power, and sputtering time, were optimized for the TiN deposition process. Pulse laser deposition was used to prepare film through COMPex 201 excimer laser. The schematic diagram of pulse laser deposition is shown in Fig. 1b. TiN with 99.9% purity was used as the target and the fixed laser frequency was 8 Hz. The deposition process started when the vacuum degree of the chamber reached 2×10^{-4} Pa. The deposition process parameters of TiN were optimized, including N_2 partial pressure, substrate temperature, and deposition duration. The specific sedimentary parameters are shown in Table 2.

Table 1 Element composition and content of TA1 plate (wt%)

Al	Mn	Fe	C	N	H	O	Ti
0.7–2.0	0.3	0.08	0.05	0.012	0.015	0.1	Bal.

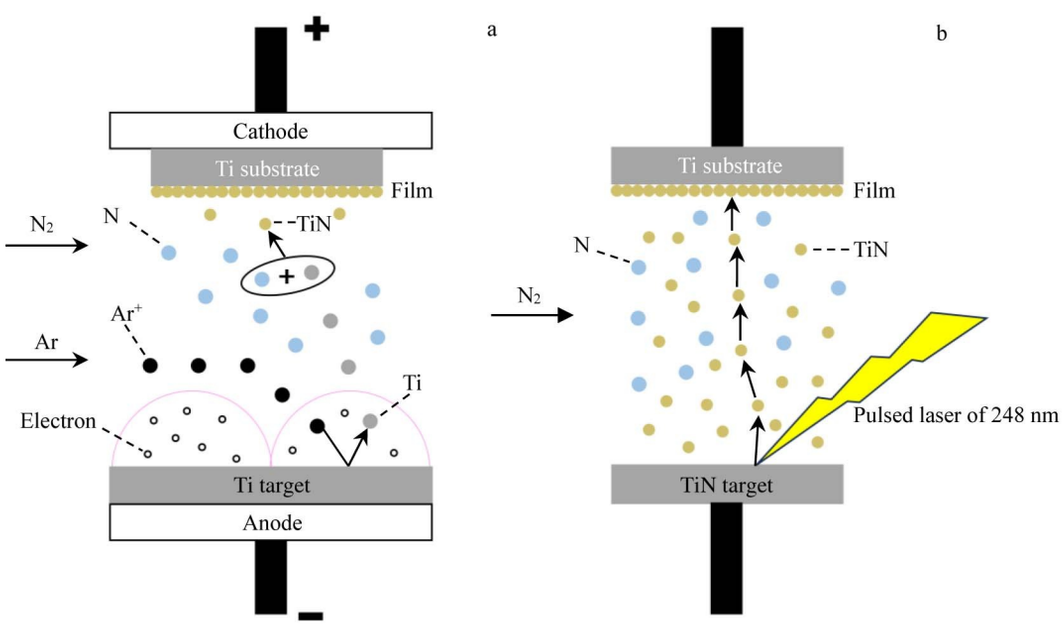

Fig.1 Schematic diagrams of magnetron reactive sputtering (a) and pulse laser deposition (b) processes for TiN film preparation

Table 2 Process parameters for TiN film preparation

Parameter	Magnetron reactive sputtering	Pulsed laser deposition
N_2 flow rate/mL·min^{-1}	2, 4, 6, 8	-
Partial pressure/Pa	-	0, 2, 4, 6
Sputtering power/W	80, 90, 100, 110, 120	-
Substrate temperature/°C	25, 100, 200, 300, 400	25, 200, 400, 600
Reaction time	1.5 h, 2.5 h, 3.5 h	1000 s, 2000 s, 3000 s, 4000 s

The morphology analysis of the prepared film was conducted by FEI-VERIOS 460 scanning electron microscope (SEM) and OLYMPUS OLS51-SU confocal laser scanning microscope (CLSM). The phase structure was characterized by the Netherlands Malvern Panalytic Empire X-ray diffractometer (XRD). The analysis of the valence states of elements from the film surface was conducted by Thermo Fisher ESCALAB Xi^+ X-ray photoelectron spectrometer (XPS).

Electrochemical performance test was conducted with three-electrode system on Autolab electrochemical workstation. The working electrode was the modified Ti plate with an exposed working area of 1 cm^2. The counter electrode was platinum mesh, and the reference electrode was saturated calomel electrode (SCE). The electrolyte was composed of 0.5 mol/L H_2SO_4 and 2×10^{-4}wt% F^- and its test temperature was 80 °C. The samples were soaked in the open circuit for 1 h to measure the stable open circuit voltage. To test the dynamic response of the samples under the working potential condition and the effect of potential on the corrosion resistance, the potentiodynamic polarization tests of the samples were performed from −1 V vs. SCE to 2 V vs. SCE. All potential data measured for analysis were based on SCE as reference electrodes with the scanning speed of 1 mV·s^{-1}. For simple description, the unit of V vs. SCE is also denoted as V. The data such as corrosion potential and corrosion current density could be obtained by Tafel fitting of the results. Under constant potential test, the stability was verified by maintaining the voltage at 2 V for 3 h.

The contact angle measurement was conducted by the German KRUSS droplet imaging analyzer. The samples were placed horizontally on the observation table firstly, and then a drop of distilled water was fell on the surface. The software captured the droplet image, selected the horizontal plane, and automatically obtained the contact angle value. The contact angle could reflect the hydrophilicity of the sample surface. The larger the contact angle, the stronger the hydrophobicity, which is more conducive to the drainage of PEMWE stack during service.

2 Results and Discussion

2.1 Topography characterization

After process optimization, the optimal reaction conditions for TiN film preparation through magnetron reactive sputtering were determined: N_2 flow rate of 6 mL/min, sputtering power of 100 W, substrate temperature of 300 °C, and processing duration of 2.5 h. In this case, the sample was named as 1#TiN. The optimal reaction conditions for TiN film preparation through pulse laser deposition were N_2 partial pressure of 2 Pa, substrate temperature of 400 °C, and duration of 2000 s. In this case, the sample was named as 2#TiN.

Fig.2 shows SEM images and surface roughness results of 1#TiN and 2#TiN samples. It can be seen that both 1#TiN and

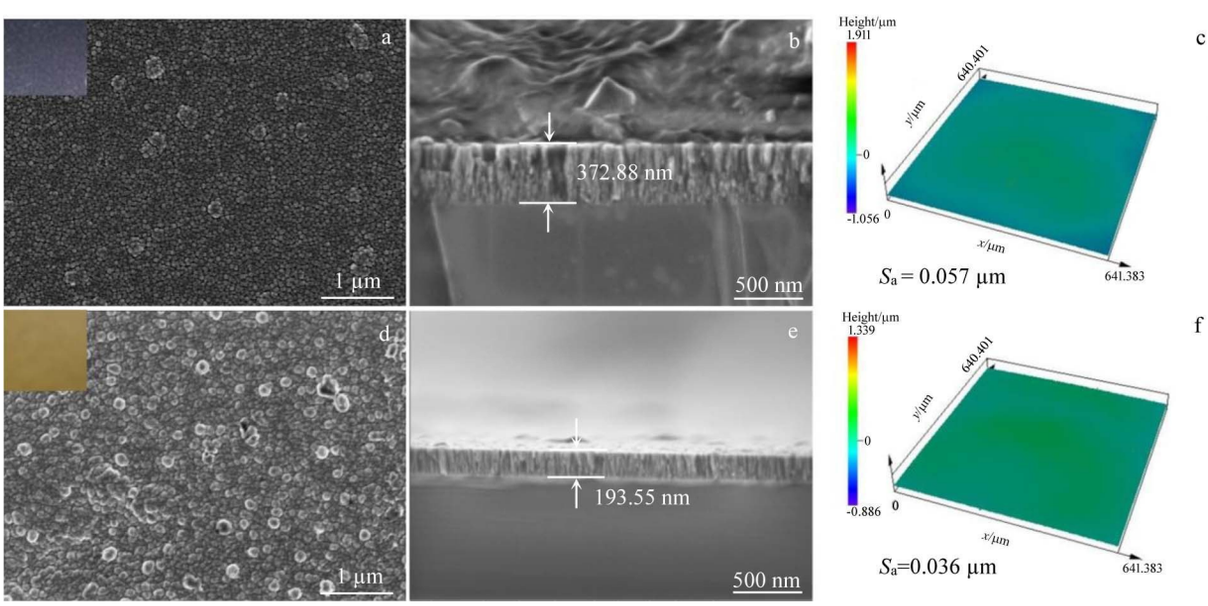

Fig.2 SEM surface (a, d) and cross-section (b, e) images as well as surface roughness results (c, f) of 1#TiN (a–c) and 2#TiN (d–f) samples

2#TiN sample surfaces are flat, dense, and uncracked with uniform grain distributions. Additionally, 1#TiN sample is grayish purple with rounded spherical grains and certain pores between the grains. The cross-section of 1#TiN sample is arranged compactly in a columnar crystal pattern, and its thickness is 372.88 nm, as shown in Fig.2b. 2#TiN sample has a yellow metallic luster with tightly connected irregular spherical grains. The columnar crystal size of the 2#TiN cross-section is finer than that of 1#TiN cross-section, the arrangement is more compact, and the thickness is 193.55 nm (Fig. 2d). Surface roughness of the samples was analyzed by the CLSM. It can be seen from Fig. 2c and 2f that the roughness of the sample surface within a large region of 640 μm×640 μm is less than 60 nm, indicating that the film surface is smooth and dense. Besides, the roughness of 1#TiN sample is greater than that of 2#TiN sample. This may be because the magnetron reactive sputtering involves multiple processes, such as sputtering, reaction, and deposition. The more the complex reaction steps and related process parameters, the rougher the surface.

2.2 Characterization of phase and composition

To confirm the phase composition and crystal structure of the film, XRD and XPS analyses were conducted on the prepared film. Fig. 3a shows XRD patterns of 1#TiN and 2#TiN samples. After the comparison with the standard PDF card, it can be concluded that the peak positions of both 1#TiN and 2#TiN samples match those of the face-centered cubic TiN phase (#PDF 38-1420), proving that the prepared film is TiN. The position of the diffraction peak of 1#TiN sample slightly shifts to the right side, compared with the standard card, indicating the increase in diffraction angle and the decrease in interplanar spacing. This may be attributed to the interference of oxygen doping. Besides, the diffraction peak intensity of 1#TiN sample is lower than that of 2#TiN sample, indicating that the crystallinity of 1#TiN sample is worse than that of 2#TiN sample. 1#TiN sample exhibits the (200) preferred crystal plane orientation, whereas 2#TiN sample exhibits multi-directional growth of (111) and (200) crystal planes.

XPS spectra of the full-scale of 1#TiN and 2#TiN samples are shown in Fig. 3b. Except for the characteristic peaks of C 1s, both 1#TiN and 2#TiN samples exhibit the characteristic peaks of Ti 2p, N 1s, and O 1s. As shown in Fig.3c, the Ti 2p spectra of 1#TiN sample can be fitted by four dominant peaks, corresponding to the characteristic energy of Ti-N (455.25 and 461.24 eV) and Ti-O (458.15 and 463.91 eV). The Ti 2p spectra of 2#TiN sample can also be fitted by four dominant peaks, corresponding to the characteristic energy of Ti-N (455.13 and 460.90 eV) and Ti-O (458.12 and 463.84 eV), which are in agreement with the results in Ref. [26], suggesting the existence of TiN and TiO_2 on the film surface of the samples. The existence of Ti-O is due to the presence of trace oxygen participating in the reaction in high-vacuum environment. Besides, the exposed film surface can be partially oxidized. The TiO_2 content of 1#TiN sample is significantly higher than that of 2#TiN sample, because during magnetron reactive sputtering, oxygen in the environment preferentially reacts with the splashed Ti, whereas the pulse laser deposition uses TiN target and hardly involves competitive reaction processes. As shown in Fig. 3d, the binding

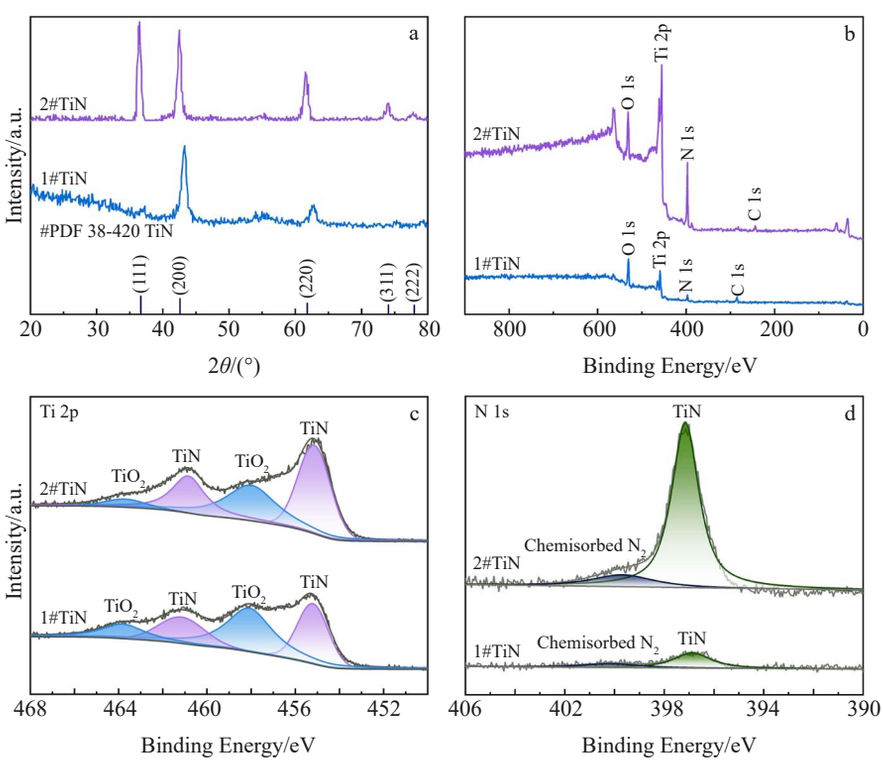

Fig.3 XRD patterns (a) and XPS spectra (b–d) of 1#TiN and 2#TiN samples: (b) full-scale, (c) Ti 2p, and (d) N 1s

energy of 1#TiN sample at 396.87 eV is related to N-Ti, and there is a small peak with lower intensity at high binding energy of 400.15 eV, which may be related to N_2 adsorption[27]. The binding energy of 2#TiN sample at 397.15 eV is also related to N-Ti, and that at 399.70 eV is related to N_2 adsorption. These results are consistent with the results in Ref. [28]. According to Fig. 3c–3d, the Ti 2p and N 1s peaks of 1#TiN sample shift towards the lower binding energy side, compared with those of 2#TiN sample, which may be due to the influence of heteroatoms during the magnetron reactive sputtering process, resulting in defects, changes in oxidation state, and impurity doping on the sample surface. These factors may lead to the decrease in binding energy, inferring the decrease in the energy of electrons from the core state to the conduction or valence band.

2.3 Corrosion resistance

The effect of different process parameters on the corrosion resistance of TiN film samples was analyzed. The test environment was simulated through the three-electrode system, and the action potential polarization curve was tested to analyze the corrosion resistance.

2.3.1 Influence of magnetron reactive sputtering parameters

Fig. 4a shows the potentiodynamic polarization curves of the samples and Ti substrate under different N_2 flow rates, and the Ar flow rate is set as 20 mL/min. The curve shows the standard electrokinetic polarization characteristic, presenting obvious activation zone, activation-passivation transition zone, and passivation zone. The experiment results show that with the increase in N_2 flow rate, the corrosion current density of the samples is firstly decreased and then increased. However, compared with that of the Ti substrate, the corrosion resistance barely improves. It is speculated that due to the poor adhesion between the film and substrate, the film reacts with the strongly acidic electrolyte and peels off during the open circuit voltage stability test. Therefore, the samples are already corroded to a certain extent before potentiodynamic polarization tests. The specific corrosion current density and corrosion potential are shown in Table 3. The optimal corrosion resistance is achieved at the N_2 flow rate of 6 mL/min with the corrosion current density of about 427.2 $\mu A \cdot cm^{-2}$, but this result is even worse than that of the Ti substrate. This may be due to the loose structure and poor crystallinity of the prepared film. When the N_2 to Ar ratio is low and the amount of introduced N_2 gas is too small, metallic sputtering occurs. However, when the N_2 to Ar ratio is high and the amount of introduced N_2 is too large, the ratio of Ti to N in the sample will not be 1:1. Different N_2 to Ar ratios will directly affect the lattice structure of the film, and the properties of TiN film with different lattice structures also vary greatly. Therefore, a suitable N_2 flow rate is a prerequisite for the sputtering of high-quality corrosion-resistant film[29–30].

Fig. 4b shows the effect of substrate temperature on the corrosion resistance of TiN films. With the increase in substrate temperature, the corrosion current density of the prepared films is firstly decreased and then increased. The optimal corrosion current density is obtained at 300 °C as 75.09 $\mu A \cdot cm^{-2}$, which is about one-fifth of the corrosion current density at 25 °C. Additionally, the activation-passivation transition zone of the film prepared at 300 °C significantly narrows, indicating an increase in passivation rate.

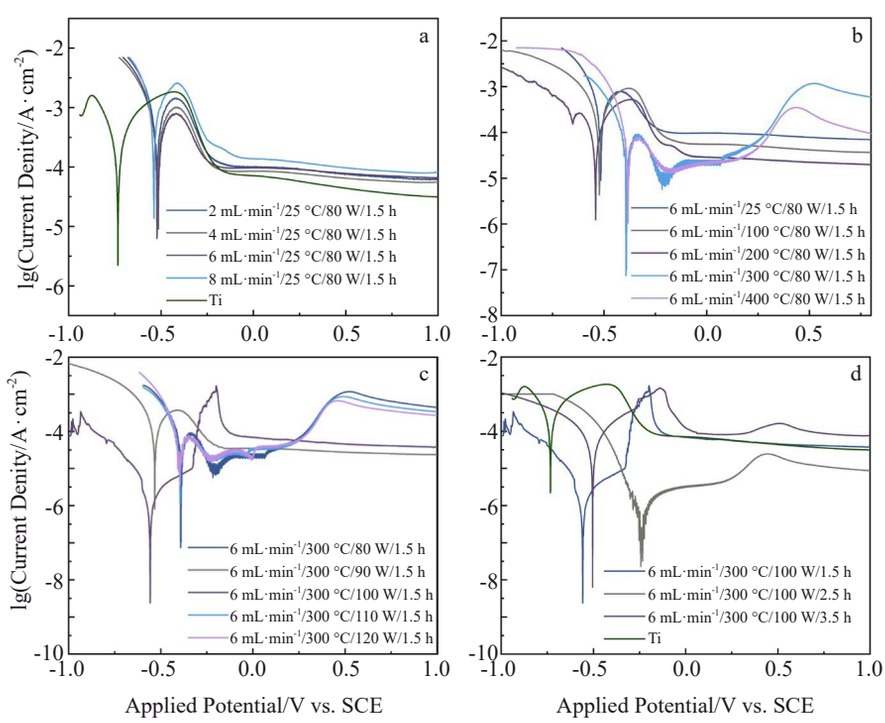

Fig.4 Potentiodynamic polarization curves of TiN films prepared by magnetron reactive sputtering with different N_2 flow rates (a), different substrate temperatures (b), different sputtering powers (c), and different sputtering durations (d)

Table 3 Corrosion potentials and corrosion current densities of TiN films prepared by magnetron reactive sputtering with different processing parameters

Processing parameter	Corrosion potential, E_{corr}/V	Corrosion current density, I_{corr}/μA·cm^{-2}
Original (Ti substrate)	−0.733	238.30
2 mL·min^{-1}/80 W/1.5 h/25 °C	−0.522	652.70
4 mL·min^{-1}/80 W/1.5 h/25 °C	−0.520	466.80
6 mL·min^{-1}/80 W/1.5 h/25 °C	−0.516	427.20
8 mL·min^{-1}/80 W/1.5 h/25 °C	−0.540	963.80
6 mL·min^{-1}/80 W/1.5 h/100 °C	−0.523	260.70
6 mL·min^{-1}/80 W/1.5 h/200 °C	−0.541	113.30
6 mL·min^{-1}/80 W/1.5 h/300 °C	−0.390	75.09
6 mL·min^{-1}/80 W/1.5 h/400 °C	−0.383	91.64
6 mL·min^{-1}/90 W/1.5 h/300 °C	−0.484	67.59
6 mL·min^{-1}/100 W/1.5 h/300 °C	−0.558	1.54
6 mL·min^{-1}/110 W/1.5 h/300 °C	−0.398	56.40
6 mL·min^{-1}/120 W/1.5 h/300 °C	−0.397	70.94
6 mL·min^{-1}/100 W/2.5 h/300 °C	−0.246	0.59
6 mL·min^{-1}/100 W/2.5 h/300 °C	−0.504	40.72

This should mainly be due to the amelioration of surface defects and pores of the film structure caused by the increase in substrate temperature. This is because increasing the substrate temperature can enhance the migration and diffusion rates of atoms, thereby forming a smooth surface film. When the substrate temperature is low, the critical nuclear size of the film is small, and new nuclei are constantly generated during the deposition process. At the same time, the migration rate of atoms on the substrate surface is slow, and the growth of internal grains is inhibited, resulting in the increase in the density of defects inside the grains and affecting the quality of the film. Furthermore, it increases the probability of electrolyte corroding on the substrate through the film[31]. Therefore, an appropriate substrate temperature is of great significance to improve the corrosion resistance of TiN film.

Fig.4c shows the effect of sputtering power on the corrosion resistance of TiN films. With the increase in sputtering power, the corrosion current density of the prepared films is firstly decreased and then increased. The optimal corrosion current density is achieved at 100 W as 1.54 μA·cm^{-2}, which is about one-fifth of the corrosion current density at 80 W. The range of activation-passivation transition zone on the film prepared at 100 W further narrows, and correspondingly, the stable rate of passivation behavior is significantly improved. This should mainly be due to the less surface accumulation and defects as well as the lower roughness. If the power is very low, the atoms possess a little energy, and their migration rate on the substrate will be slow, resulting in the uneven growth of thin film and affecting the film performance. Additionally, in this case, the atomic deposition rate of the target material will be slow, which is easily affected by other atoms in the chamber during sputtering, thereby influencing the uniformity of film composition and ultimately affecting the film deposition quality[32]. Therefore, appropriate power is crucial to maintain high corrosion-resistant components and structure.

Fig. 4d shows the effect of sputtering duration on the corrosion resistance of TiN films. With the prolongation of sputtering duration, the corrosion current density of the prepared films is firstly decreased and then increased. The film prepared for 2.5 h does not have obvious activation-passivation transition zone, and the passivation behavior is further accelerated and becomes stable. The optimal corrosion current density is about 0.59 μA·cm^{-2}, which is about one-third of the corrosion current density of film prepared for 1.5 h. The corrosion potential also increases to −0.246 V, which should be mainly attributed to the uniform density of its structure and the reduction in pores. With the prolongation of sputtering duration, individual grains further grow and coalesce, forming larger and more compact grains with a tighter film structure. Prolonging the sputtering duration allows for wider interconnection and overlap of grains to form continuous film with reduced porosity. However, it also increases the occurrence probability of defects and impurities, affecting the corrosion resistance of the films[33]. Therefore, selecting appropriate sputtering duration has an undeniable impact on the preparation of dense corrosion-resistant films.

2.3.2 Influence of pulse laser deposition parameters

Fig. 5a shows the effect of N_2 partial pressure on the corrosion resistance of TiN films prepared by pulse laser deposition, and the results are listed in Table 4. The substrate exhibits poor corrosion resistance, but after modification with TiN film prepared by pulse laser deposition, the corrosion resistance significantly improves. The polarization curve of dynamic potential exhibits obvious characteristics of activation zone, activation-passivation transition zone, and passivation zone. With the increase in N_2 partial pressure, the corrosion current density shows a trend of first decreasing and then increasing. When the N_2 partial pressure is 2 Pa, the

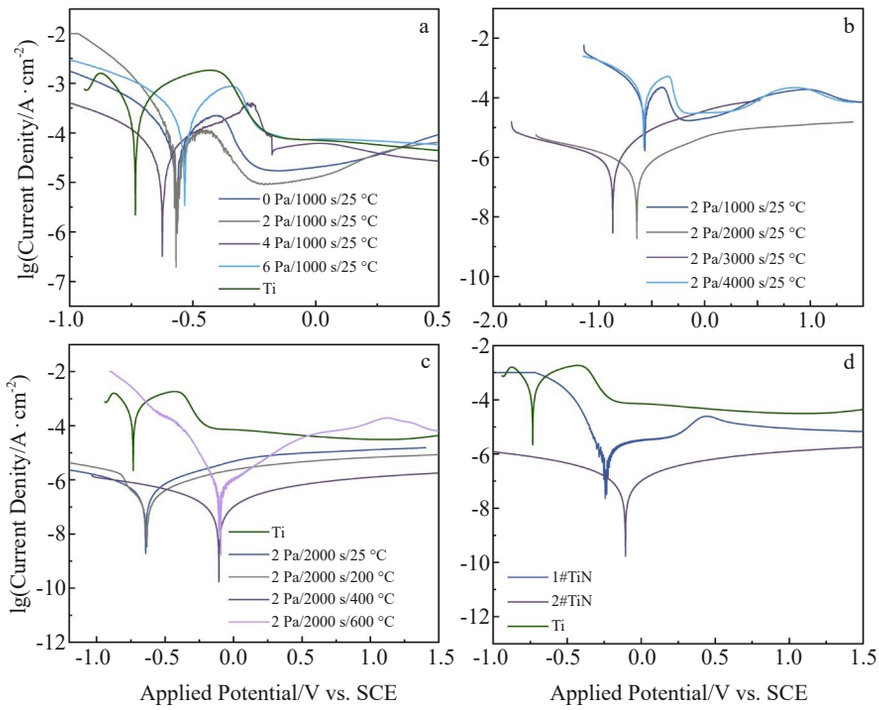

Fig.5 Potentiodynamic polarization curves of TiN films prepared by pulse laser deposition with different N_2 partial pressures (a), different deposition durations (b), and different substrate temperatures (c); comparison of potentiodynamic polarization curves of 1#TiN film, 2#TiN film, and Ti substrate (d)

corrosion current density of the TiN film is 5.678 μA·cm^{-2}, which is about one-sixtieth of that of the Ti substrate. This verifies the feasibility of pulse laser deposition to prepare TiN film in order to modify Ti bipolar plate for corrosion resistance enhancement. When the N_2 partial pressure is high, the average free path of atoms is small, and the probability of collisions between atoms is high, which reduces the deposition rate and leads to excessive energy loss when the atoms reach the substrate surface. Therefore, their migration ability on the substrate is degraded, lowering the film performance. Under low N_2 partial pressure, the average free path of atoms is large, and the probability of collisions between atoms greatly reduces. The high migration ability upon reaching the substrate surface is to some extent beneficial to the formation of a flat surface of the films[34]. Therefore, appropriate partial pressure is a necessary prerequisite for deposition of high-quality corrosion-resistant films.

Fig. 5b shows the effect of deposition duration on the corrosion resistance of TiN films. With the prolongation of deposition duration, the corrosion current density of the film shows a trend of firstly decreasing and then increasing. When the deposition duration is 2000 s, the corrosion current density reaches the lowest of 0.121 μA·cm^{-2}, which is about one-fiftieth of that when the deposition duration is 1000 s. There is no obvious activation-passivation transition zone in the dynamic potential polarization curve, indicating that its passivation behavior is fast and stable. It is known that the effect of deposition duration on corrosion resistance mainly depends on the defect ratio and surface smoothness of the film. Prolonging deposition duration is beneficial to the formation of larger and more compact grains as well as tighter membrane structure, but it also increases the probability of defects and impurities. Therefore, selecting appropriate deposition duration also has an undeniable impact on the preparation of dense corrosion-resistant films, which can reduce the channels for electrolyte to penetrate the substrate through the films.

Fig. 5c shows the effect of substrate temperature on the corrosion resistance of TiN films. With the increase in substrate temperature, the corrosion current density of the films shows a trend of firstly decreasing and then increasing. When the substrate temperature is 400 °C, there is no obvious activation-passivation transition zone, indicating that the passivation rate is fast and the passivation behavior is stable. The corrosion current density achieves the lowest value of 0.025 μA·cm^{-2}, which is about one-fifth of the corrosion current density when the substrate temperature is 25 ° C, indicating a significantly reduced corrosion rate from the dynamic perspective. At the same time, the corrosion potential significantly increases from −0.642 V (25 °C) to −0.106 V, indicating the improved corrosion resistance. Therefore, the film prepared under the 2 Pa/2000 s/400 °C condition has the optimal corrosion resistance. Compared with that of the Ti substrate, the corrosion current density decreases by 4 orders of magnitude. The influence of substrate temperature on the corrosion resistance mainly depends on the grain size and film structure. Proper substrate temperature can enhance the migration and diffusion rates of atoms, thereby improving the

Table 4 Corrosion potentials and corrosion current densities of TiN films prepared by pulse laser deposition with different processing parameters

Processing parameter	Corrosion potential, E_{corr}/V	Corrosion current density, I_{corr}/μA·cm^{-2}
Original (Ti substrate)	−0.733	238.300
0 Pa/1000 s/25 °C	−0.570	33.651
2 Pa/1000 s/25 °C	−0.570	5.678
4 Pa/1000 s/25 °C	−0.615	17.061
6 Pa/1000 s/25 °C	−0.532	130.86
2 Pa/2000 s/25 °C	−0.642	0.121
2 Pa/3000 s/25 °C	−0.868	0.447
2 Pa/4000 s/25 °C	−0.575	81.997
2 Pa/2000 s/200 °C	−0.634	0.089
2 Pa/2000 s/400 °C	−0.106	0.025
2 Pa/2000 s/600 °C	−0.108	0.768

surface smoothness of the film, reducing the internal defect density, and increasing the mechanical barrier effect of the film on the electrolyte. Hence, the substrate temperature has an important impact on the corrosion resistance enhancement of Ti bipolar plate substrate modified by TiN film prepared by pulse laser deposition.

Fig. 5d shows the corrosion resistance of the Ti substrate and TiN films by magnetron reactive sputtering (1#TiN) and pulse laser deposition (2#TiN). The corrosion resistance of the Ti substrate is significantly improved after TiN film modification. The passivation behavior of both films is fast and stable without obvious activation-passivation transition zone. Specifically, the corrosion current density of 1#TiN film reaches 0.59 μA·cm^{-2}, and that of 2#TiN film reaches 0.025 μA·cm^{-2}, which is higher than that of the Ti substrate (238.3 μA·cm^{-2}) by 3 and 4 orders of magnitude, respectively. From the dynamic perspective, it can be observed that the lower the current corrosion density, the lower the corrosion rate. At the same time, from the thermodynamic perspective, the higher the corrosion potential, the more difficult the corrosion occurrence. The corrosion potential of the Ti substrate, 1#TiN film, and 2#TiN film is − 0.733, − 0.246, and − 0.106 V, respectively. It can be seen that the corrosion potential significantly increases after TiN film modification. Briefly, TiN films prepared by magnetron reactive sputtering or pulse laser deposition can improve the corrosion resistance of the Ti bipolar plate and provide better protection effect. The TiN film prepared by pulse laser deposition has superior corrosion resistance due to its advantages of better surface smoothness and more uniform composition.

2.4 Potentiostatic polarization

The potentiostatic polarization tests were operated for 3 h to assess the long-term corrosion behavior of the Ti substrate, 1#TiN film, and 2#TiN film in the simulated PEMWE environment. Due to the strong corrosiveness of acidic corrosive solution and high working potential, bipolar plate should maintain long-term stability. Fig. 6 shows the potentiostatic curves of Ti substrate, 1#TiN film, and 2#TiN film at 2.0 V in 0.5 mol/L H_2SO_4+2×10^{-4}wt% F^- solution, and

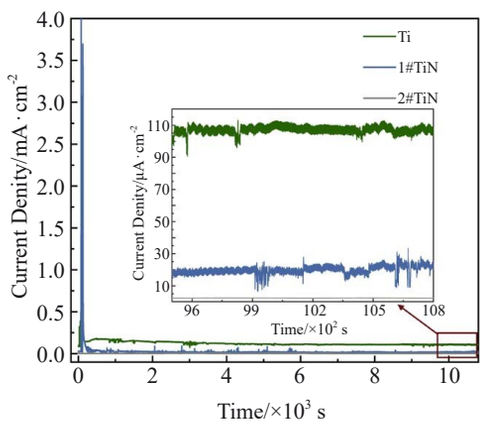

Fig.6 Potentiostatic polarization curves of Ti substrate, 1#TiN film, and 2#TiN film in simulated PEMWE environmen

Table 5 shows the corrosion current density results.

The current densities of all samples decrease rapidly and then remain at a relativity stable value due to the surface passivation. The initial current density of the Ti substrate is 85.6 μA·cm^{-2}. With the reaction of the substrate in solution, the current density of the Ti substrate is rapidly decreased followed by a brief increase and then decreases again to maintain relative stability. The original oxide layer on the surface of the Ti substrate is destroyed firstly, so the current density value of the Ti substrate rapidly increases. Then, the surface passivation occurs, the current density starts to stabilize at around 421 s and remains at about 108.146 μA·cm^{-2} after 3 h. The initial current density of 1#TiN film is 30.2 μA·cm^{-2}.

Table 5 Corrosion current densities of Ti substrate, 1#TiN film, and 2#TiN film after potentiostatic polarization at 2 V for 3 h

Sample	Corrosion current density, I_{corr}/μA·cm^{-2}
Ti substrate	108.146
1#TiN film	21.057
2#TiN film	2.270

With the reaction of 1#TiN film in the solution, due to surface passivation, the current density value of 1#TiN film rapidly decreases, then stabilizes at around 321 s, and remains at about 21.057 μA·cm^{-2} after 3 h. The initial current density of 2#TiN film is 22.6 μA·cm^{-2}. With the reaction of 2#TiN film in the solution, the current density value of 2#TiN film rapidly decreases because of the surface passivation, begins to stabilize at around 49 s, and finally remains at about 2.27 μA·cm^{-2} after 3 h.

1#TiN and 2#TiN films have lower current densities than the Ti substrate, indicating that they have good protective effects. The potentiostatic polarization curves of Ti substrate and 1#TiN film show significant fluctuations, which is possibly because the surface passivation film is not dense. Thus, obvious passivation film damage and regeneration occur. However, the potentiostatic polarization curve of 2#TiN film always maintains a stable state, indicating that 2#TiN film has better protective performance. This may be because 2#TiN film has good composition uniformity, good crystallinity, and low surface roughness. The less formation of gaps and particles in the 2#TiN film results in the better protective effect of the generated passivation layer, which is consistent with the results of the previous dynamic potential polarization curve tests.

2.5 Contact angle analysis

The hydrophobicity of the bipolar plate affects the stack drainage and the corrosion of the bipolar plate in the electrolyte. Fig. 7 shows the water contact angles of Ti substrate, 1#TiN film, and 2#TiN film. Through curve fitting analysis and calculation results, the contact angles of the Ti substrate, 1#TiN film, and 2#TiN film are 42.8°±1°, 105.5°±1°, and 107.3°±1°, respectively. After modification by TiN film, the water contact angle of the Ti substrate increases significantly. The larger the contact angle, the stronger the hydrophobicity, which is more conducive to the drainage of bipolar plate flow field and weakens the diffusion of electrolyte through film to substrate, therefore slowing down the corrosion progress. Hence, the modified samples all show excellent hydrophobicity. Particularly, 2#TiN film shows the optimal hydrophobicity, which may be due to its polycrystalline orientation, leading to the lower surface roughness[35] and affecting corrosion resistance. This is also consistent with the results of the potentiodynamic polarization curves and potentiostatic polarization curves.

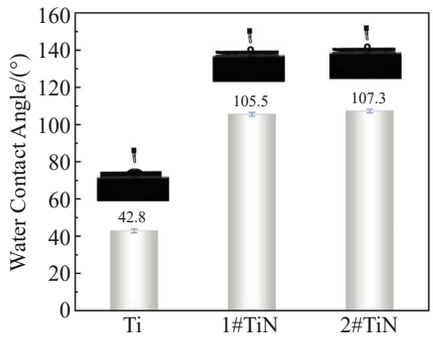

Fig.7 Water contact angles of Ti substrate, 1#TiN film, and 2#TiN film

2.6 Corrosion mechanism

Through the electrochemical behavior analysis, it is found that TiN film has excellent corrosion resistance. However, there are still significant differences among TiN films prepared under different processing conditions. To illustrate the corrosion process, Fig. 8 presents the schematic diagrams of the corrosion mechanisms of Ti substrate, 1#TiN film prepared by magnetron reactive sputtering, and 2#TiN film prepared by pulse laser deposition.

When the prepared TiN film firstly meets the electrolyte, its surface oxide layer has a certain degree of resistance against the erosion of corrosive ions, such as H^+, F^-, and SO_4^{2-} in the electrolyte. However, the stability of the oxide layer in acidic solutions is relatively low, and the oxide layer gradually dissolves over time. Subsequently, the corrosive ions in the electrolyte use the columnar crystal gaps of the film as the general channels to destroy the TiN film, and the pinholes and defects in the film are served as the fast channels, gradually dissolving the TiN film completely. Thus, the TiN film gradually fails after corrosion and dissolution, losing its protective effect, and the substrate is corroded after exposure. It is undeniable that the prepared TiN film has a physical barrier effect. 1#TiN film provides a certain anti-corrosion effect on the exposed Ti substrate surface. 2#TiN film has higher surface smoothness, stronger hydrophobicity, more uniform composition, and lower porosity, reducing the erosion

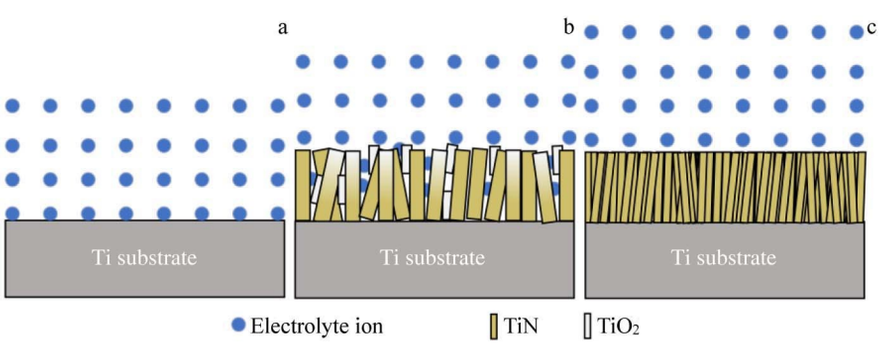

Fig.8 Schematic diagrams of corrosion mechanism of Ti substrate (a), 1#TiN film (b), and 2#TiN film (c)

degree caused by harmful ions, such as H^+, SO_4^{2-}, and F^- in the channels of TiN film, which results in better blocking effect against the inward diffusion of harmful ions in the electrolyte and better protection for the Ti substrate.

3 Conclusions

1) The optimal processing parameters of magnetron reactive sputtering for TiN film preparation are N_2 flow rate of 6 mL/min, sputtering power of 100 W, substrate temperature of 300 °C, and duration of 2.5 h. The corrosion current density reaches 0.59 μA·cm^{-2}, decreasing by 3 orders of magnitude, compared with that of the Ti substrate. For the TiN film prepared by magnetron reactive sputtering, the contact angel is 105.5°±1° and the corrosion current density is 21.057 μA·cm^{-2} after potentiostatic polarization at 2 V for 3 h.

2) The optimal processing parameters of pulse laser deposition for TiN film preparation are N_2 partial pressure of 2 Pa, substrate temperature of 400 °C, and duration of 2000 s. In this case, the corrosion resistance is optimal: the corrosion current density is 0.025 μA·cm^{-2}, decreasing by 4 orders of magnitude, compared with that of the Ti substrate. For the TiN film prepared by pulse laser deposition, the contact angel is 107.3°±1° and the corrosion current density achieves 2.27 μA·cm^{-2} after potentiostatic polarization at 2 V for 3 h.

3) TiN films prepared by magnetron reactive sputtering and pulse laser deposition can improve the corrosion resistance of PEMWE Ti bipolar plates, and the performance of TiN film prepared by pulse laser deposition is significantly better than that prepared by magnetron reactive sputtering. This is ascribed to the uniform phase and compact structure after pulse laser deposition preparation. However, the service life of the modified film should be further improved.

References

1 Feng Q, Yuan X Z, Liu G Y *et al. Journal of Power Sources*[J], 2017, 366: 33

2 Chen J Y, Zhang S M, Zheng J *et al. Journal of Alloys and Compounds*[J], 2024, 976: 173033

3 Zhai W F, Chen Y, Liu Y D *et al. ACS Nano*[J], 2023, 17(17): 17254

4 Chen Y, Liu Y D, Li L *et al. Advanced Functional Materials*[J], 2024, 34: 2406587

5 Liu Y D, Li L, Wang L *et al. Nature Communications*[J], 2024, 15: 2851

6 Wang W L, He S M, Lan C H. *Electrochimica Acta*[J], 2012, 62: 30

7 Song Y X, Zhang C Z, Ling C Y *et al. International Journal of Hydrogen Energy*[J], 2020, 45(54): 29832

8 Wilberforce T, El-Hassan Z, Ogungbemi E *et al. Renewable & Sustainable Energy Reviews*[J], 2019, 111: 236

9 Zhang D, Peng L F, Yi P Y *et al. ACS Applied Materials & Interfaces*[J], 2021, 13(3): 3825

10 Ma G S, Yuan J H, Chen R D *et al. Applied Surface Science*[J], 2022, 597: 153670

11 Tan Q Y, Wang Y L. *Corrosion Science*[J], 2021, 190: 109703

12 Peng S, Xu J, Li Z Y *et al. Ceramics International*[J], 2020, 46(3): 2743

13 Li T, Yan Z, Liu Z Z *et al. Corrosion Science*[J], 2022, 200: 110256

14 González-Gutiérrez A G, Pech-Canul M A, Chan-Rosado G *et al. Fuel*[J], 2019, 235: 1361

15 Yan P F, Ying T, Yang Y *et al. Corrosion Science*[J], 2022, 197: 110086

16 Yan P F, Ying T, Li Y X *et al. Journal of Power Sources*[J], 2021, 484: 229231

17 Nan Rong, Cai Jianhua, Yang Jian *et al. Titanium Industry Progress*[J], 2023, 40(5): 40 (in Chinese)

18 Asri N F, Husaini T, Sulong A *et al. International Journal of Hydrogen Energy*[J], 2017, 42(14): 9135

19 Xu J, Huang H J, Li Z Y *et al. Journal of Alloys and Compounds*[J], 2016, 663: 718

20 Zhang P C, Hao C M, Han Y T *et al. Surface & Coatings Technology*[J], 2020, 397: 126064

21 Zhao Q P, Mou Z X, Zhang B *et al. Diamond and Related Materials*[J], 2020, 102: 107692

22 Wang S H, Peng J, Lui W B *et al. Journal of Power Sources*[J], 2006, 162(1): 486

23 Shi J F, Zhang P C, Han Y T *et al. International Journal of Hydrogen Energy*[J], 2020, 45(16): 10050

24 Gao Zhengyuan, Huang Naibao, Shao Zhigang *et al*. *Chinese Journal of Power Sources*[J], 2019, 43(10): 1690 (in Chinese)

25 Hu Z Y, Yuan L, Luo H *et al*. *Steel Research International*[J], 2023, 94(8): 230089

26 Cheng Y, Zheng Y F. *Surface & Coatings Technology*[J], 2007, 201(9–11): 4909

27 Jin J, Hu M L, Zhao X H. *International Journal of Hydrogen Energy*[J], 2020, 45(43): 23310

28 Jin J, Zhang J Z, Hu M L *et al. Corrosion Science*[J], 2021, 191: 109757

29 Wang Xiaohan, He Qianmei, Lu Zheng *et al. Chinese Science Bulletin*[J], 2019, 64(20): 2127 (in Chinese)

30 Jiang X, Wu Y X, Qi J W *et al. Vacuum*[J], 2024, 220: 112829

31 Li H W, Huang H F, Lina A *et al. Heliyon*[J], 2024, 10(1): e23349

32 Xie Y P, Sun Q Y, Hu Y C *et al. Vacuum*[J], 2024, 219: 112678

33 Ahmed F M, Ali A M M, Ismail R A *et al. Journal of Materials Science-Materials in Electronics*[J], 2023, 34(27): 1906

34 Liu Z C, Liang J S, Zhou H *et al. Applied Surface Science*[J], 2023, 608: 155292

35 Jiang Lei. *Chemical Industry and Engineering Progress*[J], 2003, 22(12): 1258 (in Chinese)

TiN薄膜增强改性钛双极板耐蚀性能

邓真桢[1]，戴正飞[1]，伍维博[1]，来睿思[1]，冯　庆[2]，贾　波[2]，王　琛[1]，吕源江[1]，马　飞[1]

(1. 西安交通大学 金属材料强度国家重点实验室，陕西 西安 710049)

(2. 西安泰金工业电化学技术有限公司，陕西 西安 710021)

摘　要：为了提高钛双极板的耐蚀性能，采用磁控反应溅射技术和脉冲沉积技术在商业纯钛TA1表面制备了氮化钛（TiN）薄膜，并对不同工艺参数下制备的薄膜进行了评价。结果表明，在不同制备工艺下TA1表面均可以形成致密完整的TiN膜，并显著提高钛基体的腐蚀电流密度。其中，磁控反应溅射所制备的薄膜成分受到氧气竞争反应的影响，其均一性低于脉冲激光沉积所制备的薄膜，脉冲激光沉积制备的薄膜在低腐蚀电流密度（0.025 μA·cm^{-2}）、中等腐蚀过电位（–0.106 V）和良好的疏水性方面具有更优异的综合性能。

关键词：质子交换膜水电解槽；双极板；工艺参数；TiN薄膜；耐蚀性能

作者简介：邓真桢，女，2000年生，硕士，西安交通大学金属材料强度国家重点实验室，陕西 西安 710049，E-mail：dzz1028@stu.xjtu.edu.cn